https://doi.org/10.2352/ISSN.2169-4451.2017.32.406

Regenerated silk fibroin as an inkjet printable biomaterial

Yu Zhang[1], David A. Gregory[1], Patrick J. Smith[2] and Xiubo Zhao[1];[1]Department of Chemical and Biological Engineering, University of Sheffield, Mapping Street, S1 3JD, Sheffield, UK; [2]Department of Mechanical Engineering, University of Sheffield, 64 Garden Street, S1 4BJ, Sheffield, UK;

Abstract

Regenerated silk fibroin (RSF) protein is an FDA approved biomaterial and has been used as a bio-ink to fabricate structures using inkjet printing. Silk can be present in water soluble amorphous (Silk I) and water insoluble crystalline conformations (Silk II) made up of beta-sheet structures. Here we show the generation of silk scaffolds by inkjet printing of water soluble RSF inks and then converting them into insoluble beta-sheet (Silk II) structure via a second ink containing methanol. This paper focuses on optimising printing conditions of RSF bio-ink through establishing the relationships between RSF peptide concentrations, number of layers and the total thickness of the printed layers. Various patterns such as dot arrays, lines, films, particles and logos have successfully been fabricated. The emerging of inkjet printing of RSF ink allows us to print delicate silk scaffold patterns for different applications specifically in biomedical field.

Introduction

The increasing morbidity and the limited supply of donors require tissue engineering (TE) as a treatment of organ failures.[1] The TE method involves regenerating tissues within suitable scaffolds with the aim of transplanting the artificial structured tissues to the target site. These constructed scaffolds require high biocompatibility, tailorable biodegradability and good mechanical properties. Materials like metals, polymers, and ceramics, are widely used to fabricate these scaffolds.[2] Among these materials, a natural biomaterial, regenerated silk fibroin (RSF), is of interest because of its water-based preparation process and remarkable properties such as good biocompatibility, tailorable biodegradability and good mechanical properties.[3-6]

With the development of novel approaches for biomaterial fabrication, TE scaffolds are more convenient to be built up than before. In the past three decades, electrospinning was used to fabricate fibrous TE scaffolds.[7] However, electrospinning has a number of fundamental problems remaining unsolved, such as the suitable viscosity of the solution for spinning process still cannot be controlled.[7] Nowadays, inkjet printing has emerged as the most attractive direct patterning technique for versatile designs. It is convenient to fabricate tissue scaffolds as it is fully digitally driven with a computer.[8]

Using *Bombyx mori* (*B. mori*) silk as the base biomaterials, an RSF aqueous solution was developed and used as an ink for inkjet printing. The key ink property is its ability to form single droplets. Generally, the most important physical properties to take into account when determining the printability of an ink are density (ρ), surface tension (γ), viscosity (η) and nozzle diameter (d).[9-12] According to the Navier-Stokes equation, these physical properties can be used to evaluate the inertial force, capillary force and viscous force for forming stable droplet by a number of dimensionless groupings of physical constants.[10, 13] The most useful constants are the Reynolds (*Re*), Weber (*We*) and inverse (*Z)* of Ohnesorge (*Oh*) numbers:

$$Re = (v\ \rho\ D) / \eta \quad (1)$$

$$We = (v^{\wedge 2}\ \rho\ D) / \gamma \quad (2)$$

$$Z = 1 / Oh = Re / We^{1/2} = (\gamma\ \rho\ D)^{1/2} / \eta \quad (3)$$

The earliest important work trying to understand the mechanisms of drop generation was reported by Fromm who identified the *Oh* and proposed that $Z > 2$ for stable drop generation.[9] Then, Reis and Derby refined *Z* of the printable solution to be in the range of 1 to 10. [10] When *Z* is too low, viscous forces are dominant, which requires large pressure for ejection; contrary, if *Z* is too high a continuous column is ejected that can result in satellite droplets forming alongside the main drop. Later, Jang et al.[11] redefined the printable range as $14 \geqslant Z \geqslant 4$ by considering characteristics such as position accuracy, maximum allowable jetting frequency, and single-drop formability. Jang et al. recognized that the lower limitation of Z is controlled by the dissipation of the pressure pulse by fluid viscosity, and the upper limit of Z is governed by the point at where a satellite forms instead of a single droplet.

However, several groups reported stable inkjet printing even for $4 > Z > 1$ and $Z < 14$. Liu et al. [12] illustrated that $Z > 14$ ink can produce single droplet with a double waveform by adding extra negative pressure to avoiding satellite droplets.

This paper focuses on demonstrating the printability of the RSF inks and optimizing printing conditions of RSF bio-ink through establishing the relationships between RSF peptide concentrations, number of layers and the total thickness of the printed scaffolds. Various patterns such as dot arrays, lines, films, particles and complex logos, for example 'SHEFFIELD ENGINEERING', have successfully been fabricated. In the future, these inks can be formulated by adding other components such as growth factors, enzymes, particles, and other functional materials to fabricate various tissue engineering scaffolds that can meet different requirements of the end uses.[14-17]

Materials and Methods

The preparation of RSF inks is a water-based process (Figure 1). In this research, the Ajisawa's method (this method used Ajisawa's reagent to dissolve silk fibroin. A reagent mixed of $CaCl_2$ / Ethanol / Water = 1:2:8 molar ratios) was used to dissolve silk fibroin. [18] Briefly, silk from *B. mori* was degummed in order to remove sericin. Raw silk was added in 0.02 M boiling sodium Carbonate (Na_2CO_3) solution for 30 minutes. Then, the resulting silk materials were rinsed with deionized (DI) water until the solution was looked clear and dried in drying cabinet at 40 ℃ overnight. 2 g of the degummed fibroin was dissolved in 10 ml of the Ajisawa's reagent at 75 ℃ for 3 hours under mild stirring. The resulting RSF solution was allowed to cool down and dialysed in DI water for approximately 3 days in 12-14 kDa molecular weight cut off dialysis tubing at room temperature (22 ℃) to remove the salts. Dialysis water was changed until the electric conductivity of the dialysis solution was in close proximity to the electric

conductivity of DI water. The dialysed RSF solution was then centrifuged at 10000 rpm for 15 minutes. The supernatant solution was collected for printing as bio-ink (Figure 1).

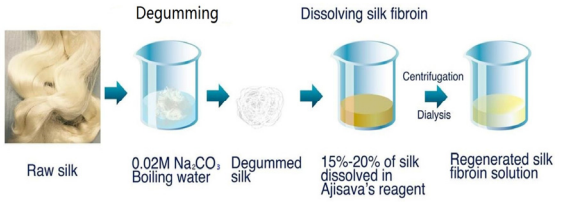

Figure 1. *Preparation of RSF solution contains three main steps which are degumming, dissolving and dialysis.*

The rheological properties of the RSF inks can be tuned within the range of γ from 40 to 75 mN/m, and between 1 and 300 mPa·s for viscosity at 21℃ by adjusting the concentration of RSF solution.

A drop-on-demand (DOD) inkjet printer (MicroFab IV, MicroFab Inc., USA) was used to conduct the printing works and a 60 µm diameter piezoelectric print head (MicroFab Inc., USA) was selected for this experiment.

Results and Discussion

Table 1 lists the physical properties of a series of different concentration of RSF solutions. The *Z* values of the 10, 20, 30 and 40 mg/ml RSF solutions are 40.9, 32.1, 25.3 and 20.3 respectively. It is worth noting that the Z values of all the inks are above 14, which mean that they require extra pressure to form stable single droplets.[12] These inks were then loaded into the printer vessel. Figure 2 shows charge-coupled device (CCD) camera caught droplets ejection images which experimental observation of droplet formation for (a) 10 mg/ml, (b) 20 mg/ml, (c) 30 mg/ml and (d) 40 mg/ml of RSF inks. It can be seen from the images that single droplets were formed, with higher concentration forming better droplets due to the lower *Z* value.

Table 1. Physical properties of RSF inks

RSF inks (mg/ml)	**0 H_2O**	**10**	**20**	**30**	**40**
ρ (Kg/m^3)	1000	1010	1020	1030	1040
η (mPa·s)	1.08	1.29	1.63	2.08	2.6
γ (mN/m)	72.9	45.96	44.76	44.65	44.73
Inverse (*Z*) of *Oh*	61.2	40.9	32.1	25.3	20.3
ρ - density; η – viscosity; γ- Surface tension; droplet diameter is 60 µm.					

Images of optical profiler microscope (Contour GT-K, USA) in Figure 3 show the morphology of 10, 20, 30 and 40 mg/ml of RSF solution printed dots. The ring structures come from the coffee-ring effect which is a result of a complex balance between outward micro-flow distribution, solution impact and different evaporation rates between the center and the edge of the deposited materials.[19, 20] The thickness (400 ±65 nm) of the edge of coffee-ring structure is higher than the thickness (100 ±30 nm) of the center area (Figure 3).

Figure 3 also shows that the higher concentration of RSF inks form smaller rings than the lower concentration of RSF inks. Therefore, the diameter of the ring pattern can be controlled by adjusting the concentration of the RSF inks (Figure 3e); as concentration increase diameter decrease.

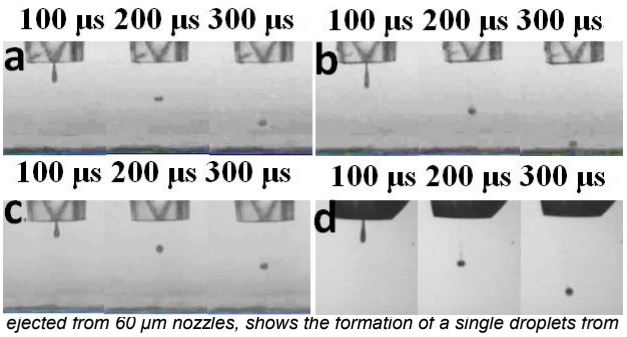

ejected from 60 µm nozzles, shows the formation of a single droplets from different concentration of RSF solutions, (a), 10 mg/ml (Z = 40.9), (b), 20 mg/ml (Z = 32.1), (c), 30 mg/ml (Z = 25.3) and (d), 40 mg/ml (Z = 20.3) respectively.

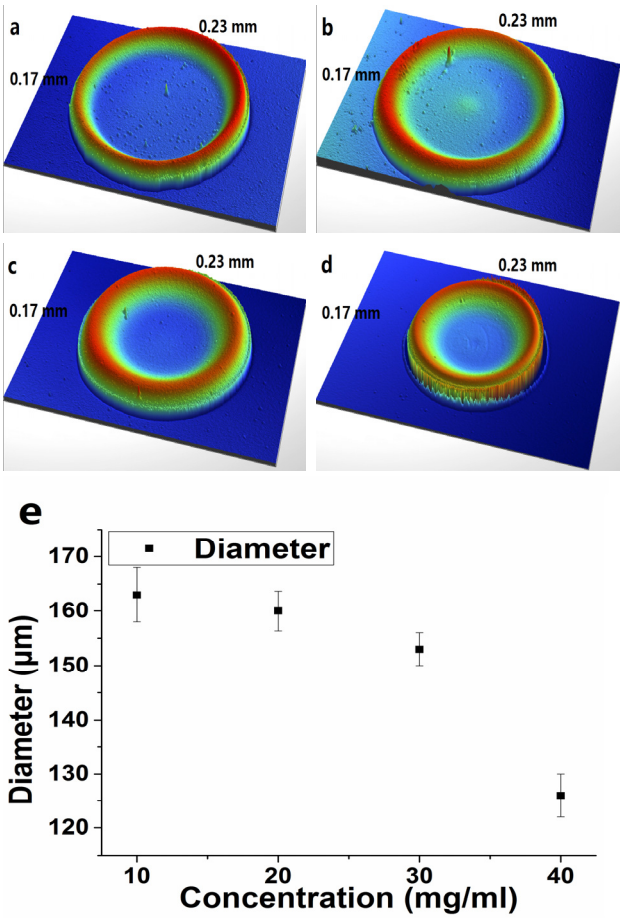

Figure 3. *Optical profiler microscope images show different concentrations of RSF solution printed dots. The concentrations are (a), 10 mg/ml, (b), 20 mg/ml, (c), 30 mg/ml and (d), 40 mg/ml respectively. e) Graph shows the diameter of the different concentrations of RSF solution printed dots.*

The choice of RSF as the main component for inkjet printing ink was not only due to its excellent biocompatibility and biodegradability[3, 4] but also due to the quick conversion of their polymorphic structure by exposing to organic solvent, which triggers the water soluble amorphous (Silk I) into water insoluble crystalline conformations (Silk II) made up of beta-sheet structures.[3] It is possible to generate silk scaffolds by inkjet printing of water soluble RSF inks and then convert it into

insoluble *beta*-sheet (Silk II) structure via a second ink containing methanol.

Changes in the structure of printed RSF films were determined by Fourier Transform Infrared (FTIR) Spectrophotometer (IRPrestige-21, Shimadzu, Japan). The infrared (IR) spectral region between 1750 cm^{-1} and 1450 cm^{-1} was classified to absorption by the peptide backbones of amide I (1700-1600 cm^{-1}) and amide II (1600-1500 cm^{-1}), which were mostly used for the analysis of different secondary structures of RSF.[21, 22] As shown in Figure 4a, the peaks at 1661-1663 cm^{-1}, 1575-1777 cm^{-1}, and 1525-1522 cm^{-1} were characteristic of silk II secondary structure, whereas the absorptions at 1672-1669 $cm^{-1}$and 1531- 1529 cm^{-1} were indicative of silk I conformation. After the printing of methanol, the peaks at 1670 cm^{-1} and 1530 cm^{-1} (silk I) decreased, whereas the peaks at 1662 cm^{-1} and 1524 cm^{-1} (silk II) increased. The results indicated that silk films with different amount of crystal structures were achieved by printing layers of methanol.

Height of printed RSF pillar prepared from 10mg/ml RSF solution is illustrated in Figure 4b (1-10 layers), 4c (20-100 layers), and 4d (200-1000 layers). Samples were prepared by printing one layer of RSF solution and followed by another layer of methanol. Evaporation of methanol leaves the silk pillars with *beta*-sheet conformation. The average thickness of each layer within 10 layers was 350 $\pm$ 50 nm, whereas that within 1000layers was 210 $\pm$ 60 nm. The difference of each layer height may be cause by the coffee ring effect which results in the height different between the edge and the center of the printed dots pattern. Above all, the more layers are printed, the higher pillars are built up. Methanol helps to form stable RSF structure which allows us to fabricate 3D scaffolds.

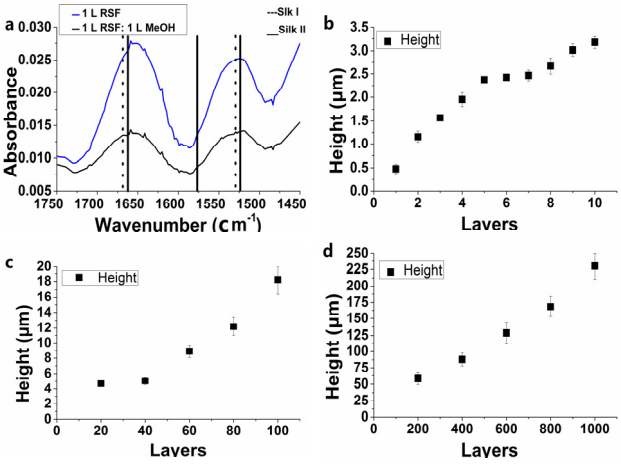

Figure 4. *(a) FTIR spectra shows silk I converting to silk II of printed RSF films after printing methanol. Thickness at edge of silk column with 10mg/ml RSF solution with different numbers of layers: (b) 1-10 layers, (c) 20-100 layers, (c) 200-1000 layers.*

In order to demonstrate the feasibility of fabricating 3 dimensional (3D) scaffolds by inkjet printing, various patterns such as dot arrays, lines, films, particles and complex logos[6], for example 'SHEFFIELD ENGINEERING', have successfully been fabricated (Figure 5). Figure 5a shows a liquid droplet can form a line by controlling the printing distance of two adjacent dots. Large printing distance (0.20 mm) between each dot makes it hard for droplets to coalesce. Droplets start to connect with each other by decreasing the distance (0.13 mm). Initial coalescence of liquid droplets forms line with periodic irregularity edge (distance between 0.12-0.03 mm). Then, after sufficient overlap (0.025 mm) a parallel-side line occurs. But if the adjacent droplets are too close to each other (0.02 mm), a bulging forms. These findings are consistent with poly (3,4-ethylenedioxythiophene) poly (styrene sulfonate) inks reported by Soltman et al.[20] Figure 5b shows alphabetical logo-'SHEFFIELD ENGINEERING'. It demonstrates that the RSF inks can be used to print complex logo with high quality. Figure 5c shows the printed pillar of 'little light ball' shape. It extends the application for inkjet printing of RSF from two dimensional to 3D direction.

Furthermore, RSF inks can be used as a base ink and formulate functional inks by mixing enzymes, nanoparticles, growth factors, and other biomaterials. The application of the functional RSF inks for making silk micro-rockets (*Reactive inkjet printing of biocompatible silk micro-rockets*) will be presented in another section of this conference.

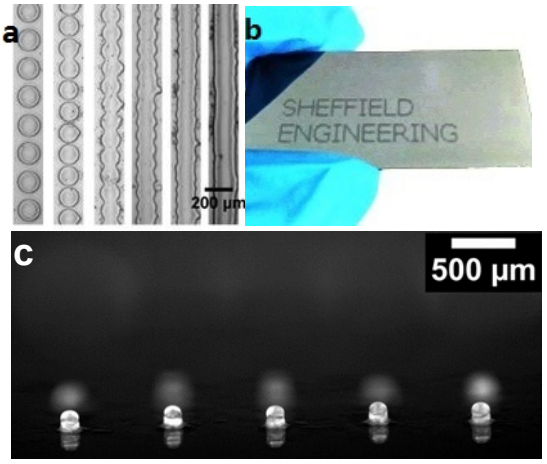

Figure 5. *Microscope images show various printed pattern. a) Lines are produced by adjusting the distance of two adjacent droplets (b) 'SHEFFIELD ENGINEERING' logo (c) The printed pillar- 'little light ball' shape*

Conclusions

To conclude, it has been demonstrated RSF solutions can be printed by inkjet printer. The printed features can be controlled by the concentration of the RSF solutions, adjusting the physical properties of RSF solutions, and post-treatment by the methanol. We also established the relationships between the number of layers and the total thickness of the printed scaffolds. Various patterns such as dot arrays, lines, films, particles and logos, have successfully been fabricated.

The growth of bio-printing provides a compelling research and development tool, and silk fibroin could play an important role as an ink material that can be formulated by adding other components such as growth factors, enzymes, particles, and other functional materials to fabricate various TE scaffolds that can meet different requirements of the end uses.

References

[1] B. Kundu, R. Rajkhowa, S. C. Kundu, and X. Wang, "Silk fibroin biomaterials for tissue regenerations," *Adv Drug Deliv Rev,* vol. 65, pp. 457-70, (2013).

[2] H. Cheung , K. Lau, T. Lu, and D. Hui, "A critical review on polymer-based bio-engineered materials for scaffold development," *Composites: Part B,* vol. 38, pp. 291-300, (2006).
[3] G. H. Altman, F. Diaz, C. Jakuba, T. Calabro, R. L. Horan, J. Chen*, et al.*, "Silk-based biomaterials," *biomaterials,* vol. 24, pp. 401-416, (2003).
[4] C. Vepari and D. L. Kaplan, "Silk as a Biomaterial," *Prog Polym Sci,* vol. 32, pp. 991-1007, (2007).
[5] Y. Wang, D. D. Rudymb, A. Walsh, L. Abrahamsend, H.-J. Kimc, H. S. Kime*, et al.*, "In vivo degradation of three-dimensional silk fibroin scaffolds," *Biomaterials,* vol. 29, pp. 3415-28, (2008).
[6] P. Rider, Y. Zhang, C. Tse, Y. Zhang, D. Jayawardane, J. Stringer*, et al.*, "Biocompatible silk fibroin scaffold prepared by reactive inkjet printing," *Journal of Materials Science, (*2016).
[7] X. Zhang, M. R. Reagan, and D. L. Kaplan, "Electrospun silk biomaterial scaffolds for regenerative medicine," *Adv Drug Deliv Rev,* vol. 61, pp. 988-1006, (2009).
[8] J. Li, F. Rossignolb, and J. Macdonald, "Inkjet printing for biosensor fabrication: combining chemistry and technology for advanced manufacturing," *Lab on a Chip,* vol. 15, pp. 2538-2558, (2015).
[9] J. E. Fromm, "Numerical-calculation of the fluid-dynamics of dropon-demand jets.," *IBM J. Res. Dev.,* vol. 28, pp. 322-333, (1984).
[10] B. Derby and N. Reis, "Inkjet printing of highly loaded particulate suspensions," *Mrs bulletin,* vol. November, pp. 815-818, (2003).
[11] D. Jang, D. Kim, and J. Moon, "Influence of Fluid Physical Properties on Ink-Jet Printability," *Langmuir,* vol. 25, pp. 2629-2635, (2009).
[12] Y. Liu, M. Tsai, Y. Pai, and W. Hwang, "Control of droplet formation by operating waveform for inks with various viscosities in piezoelectric inkjet printing," *Applied Physics a-Materials Science & Processing,* vol. 111(2), pp. 509-516, (2013).
[13] V. Bergeron, D. Bonn, J. Y. Martin, and L. Vovelle, "Controlling droplet deposition with polymer additives," *NATURE* vol. 405 (6788), p. 772, (2000).
[14] Q. Fang, D. Chen, Z. Yang, and M. Li, "In vitro and in vivo research on using Antheraea pernyi silk fibroin as tissue engineering tendon scaffolds," *Materials Science and Engineering: C,* vol. 29, pp. 1527-1534, (2009).
[15] X. Wang, T. Yucel, Q. Lu, X. Hu, and D. L. Kaplan, "Silk nanospheres and microspheres from silk/pva blend films for drug delivery," *Biomaterials,* vol. 31, pp. 1025-35, (2010).
[16] Q. Lu, B. Zhang, M. Li, B. Zuo, D. L. Kaplan, Y. Huang*, et al.*, "Degradation mechanism and control of silk fibroin," *Biomacromolecules,* vol. 12, pp. 1080-6, (2011).
[17] R. Suntivich, I. Drachuk, R. Calabrese, D. L. Kaplan, and V. V. Tsukruk, "Inkjet Printing of Silk Nest Arrays for Cell Hosting," *Biomacromolecules,* vol. 15, pp. 1428-1435, (2014).
[18] A. Ajisawa, "Dissolution of silk fibroin wieh CaCl2 ethanol H2O," *J.Seric.Sci.Jpn.,* vol. 67, pp. 91-94, (1998).
[19] O. B. Robert D. Deegan, Todd F. Dupont, Greb Huber, Sidney R. Nagel and Thomas A. Witten, "Capillary flow as the cause of ring stains from dried liquid drops," *Nature,* vol. 389 (6653), p. 827, (1997).
[20] D. Soltman and V. Subramanian, "Inkjet-Printed Line Morphologies and Temperature Control of the Coffee Ring Effect," *Langmuir,* vol. 25 (5), pp. 2224-2231, (2008).
[21] O. Shchepelina, I. Drachuk, M. K. Gupta, J. Lin, and V. V. Tsukruk, "Silk-on-silk layer-by-layer microcapsules," *Adv Mater,* vol. 23, pp. 4655-60, (2011).
[22] E. Kharlampieva, J. M. Slocik, S. Singamaneni, N. Poulsen, N. Kröger, R. R. Naik*, et al.*, "Protein-Enabled Synthesis of Monodisperse Titania Nanoparticles On and Within Polyelectrolyte Matrices," *Advanced Functional Materials,* vol. 19, pp. 2303-2311, (2009).

Author Biography

Yu Zhang received her bachelor degree in Pharmaceutical Science from Nanjing University of Technology in 2013, and is currently pursuing her PhD degree under the supervision of Dr. Xiubo Zhao at the department of Chemical and Biological Engineering, University of Sheffield. Her research is focused on inkjet printing of regenerated silk fibroin protein for medical applications.